Inorg. Chem. **2007**, *46*, 9172–9181

Reactions of *fac*-$[Re(CO)_3(H_2O)_3]^+$ with Nucleoside Diphosphates and Thiamine Diphosphate in Aqueous Solution Investigated by Multinuclear NMR Spectroscopy

Kristie M. Adams, Patricia A. Marzilli, and Luigi G. Marzilli*

Department of Chemistry, Louisiana State University, Baton Rouge, Louisiana 70803

Received May 28, 2007

Products formed between monoester diphosphates (MDPs) and *fac*-$[Re(CO)_3(H_2O)_3]OTf$ at pH 3.6 were examined. Such adducts of the *fac*-$[Re(CO)_3]^+$ moiety have an uncommon combination of properties for an "inert" metal center in that sharp NMR signals can be observed, yet the products are equilibrating at rates allowing NMR EXSY cross-peaks to be observed. Thiamine diphosphate (TDP) and uridine 5′-diphosphate (5′-UDP) form 1:1 bidentate $\{P_\alpha,P_\beta\}$ chelates, in which the MDP binds Re(I) via P_α and P_β phosphate groups. Asymmetric centers are created at Re(I) (R_{Re}/S_{Re}) and P_α (Δ/Λ), leading to four diastereomers. The two mirror pairs of diastereomers ($R_{Re}\Delta/S_{Re}\Lambda$) and ($R_{Re}\Lambda/S_{Re}\Delta$) for TDP (no ribose) and for all four diastereomers ($R_{Re}\Delta$, $R_{Re}\Lambda$, $S_{Re}\Delta$, $S_{Re}\Lambda$) for 5′-UDP (asymmetric ribose) gave two and four sets of NMR signals for the bound MDP, respectively. $^{31}P_\alpha$–$^{31}P_\alpha$ EXSY cross-peaks indicate that the *fac*-$[Re(CO)_3(H_2O)(\{P_\alpha,P_\beta\}MDP)]^-$ isomers interchange slowly on the NMR time scale, with an average $k \approx 0.8\ s^{-1}$ at 32 °C; the EXSY cross-peaks could arise from chirality changes at only Re(I) or at only P_α. Guanosine 5′-diphosphate (5′-GDP), with a ribose moiety *and* a Re(I)-binding base, formed both possible diastereomers (R_{Re} and S_{Re}) of the *fac*-$[Re(CO)_3(H_2O)(\{N7,P_\beta\}GDP)]^-$ macrochelate, with one slightly more abundant diastereomer suggested to be R_{Re} by Mn^{2+} ion ^1H NMR signal line-broadening combined with distances from molecular models. Interchange of the diastereomers requires that the coordination site of either N7 or P_β move to the H_2O site. $^{31}P_\alpha$–$^{31}P_\alpha$ EXSY cross-peaks indicate a $k \approx 0.5\ s^{-1}$ at 32 °C for R_{Re}-to-S_{Re} interchange. The similarity of the rate constants for interchange of *fac*-$[Re(CO)_3(H_2O)(\{P_\alpha,P_\beta\}MDP)]^-$ and *fac*-$[Re(CO)_3(H_2O)(\{N7,P_\beta\}GDP)]^-$ adducts suggest strongly that interchange of P_β and H_2O coordination positions accounts for the EXSY cross-peaks present in the spectra of all adducts.

Introduction

The participation of nucleotides in a large variety of biochemical processes, usually as metal ion complexes, has prompted a large number of investigations of metal-ion binding to nucleotides in solution.[1−4] Most of the literature is focused on nucleoside mono- and triphosphates. Because of the dynamic conformational changes characteristic of nucleotides and the lability of most biologically important metals such as Mg^{2+}, nucleotide coordination propensity is often assessed by using inert metal centers, which usually afford definitive results.[5−9] However, the binding of nucleoside diphosphates to metal centers has been the subject of very few studies, particularly with inert metal complexes.[8,10,11]

In recent years, the importance of Pt anticancer drugs has led to many informative investigations of Pt(II) complexes of nucleoside mono- and triphosphates.[12−16] However, the octahedral geometry is more relevant to natural biological

* To whom correspondence should be addressed. E-mail: lmarzil@lsu.edu.

(1) Lippard, S. J.; Berg, J. M. *Principles of Bioinorganic Chemistry*; University Science Books: Mill Valley, CA, 1994.
(2) Martin, R. B.; Mariam, Y. H. *Met. Ions Biol. Syst.* **1979**, *8*, 57−124.
(3) Marzilli, L. G. In *Progress in Inorganic Chemistry*; Lippard, S. J., Ed.; John Wiley and Sons: New York, 1977; Vol. 23, pp 255−278.
(4) Saenger, W. *Principles of Nucleic Acid Structure*, 1st ed.; Springer-Verlag: New York, 1984.
(5) Cleland, W. W. *Methods Enzymol.* **1982**, *87*, 159−179.
(6) Cornelius, R. D.; Cleland, W. W. *Biochemistry* **1978**, *17*, 3279−3286.
(7) Cornelius, R. D.; Hart, P. A.; Cleland, W. W. *Inorg. Chem.* **1977**, *16*, 2799−2805.
(8) Dunaway-Mariano, D.; Cleland, W. W. *Biochemistry* **1980**, *19*, 1496−1505.
(9) Lu, Z.; Shorter, A. L.; Lin, I.; Dunaway-Mariano, D. *Inorg. Chem.* **1988**, *27*, 4135−4139.
(10) Sajadi, S. A. A.; Song, B.; Gregán, F.; Sigel, H. *Inorg. Chem.* **1999**, *38*, 439−448.
(11) Bose, R. N.; Slavin, L. L.; Cameron, J. W.; Luellen, D. L.; Viola, R. E. *Inorg. Chem.* **1993**, *32*, 1795−1802.

10.1021/ic701038f CCC: $37.00
Published on Web 10/03/2007

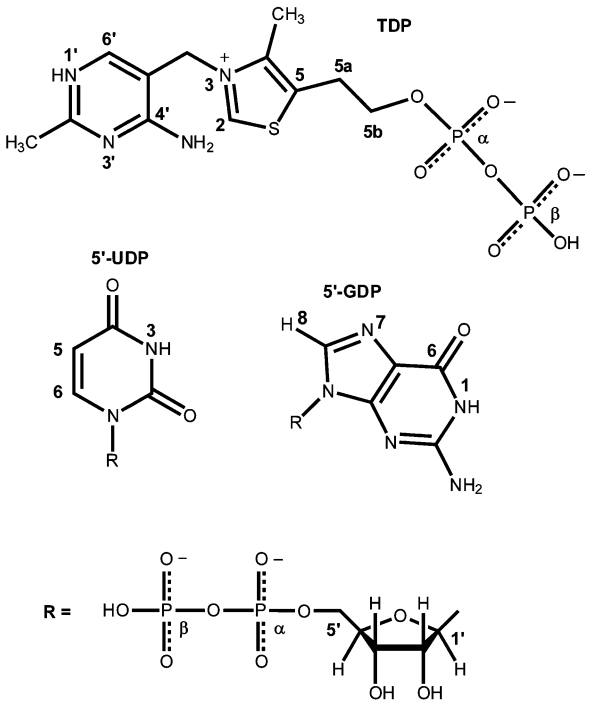

Figure 1. TDP (top). Base portion of 5′-UDP (middle left) and 5′-GDP (middle right) and the R group bearing the diphosphate moiety (bottom).

processes. More recently, we and others have recognized that the octahedral *fac*-[Re(CO)$_3$(H$_2$O)$_3$]$^+$ cation is another inert, redox-stable metal center that can be used to study metal interactions with nucleotides.[17−19] Compared to Pt(II) compounds, the *fac*-[Re(CO)$_3$(H$_2$O)$_3$]$^+$ cation may have a higher affinity for oxygen donors.[20] Previous work demonstrated that reactions of *fac*-[Re(CO)$_3$(H$_2$O)$_3$]$^+$ and nucleoside monophosphates (NMPs) attained equilibrium, forming predominantly Re/NMP 1:1 complexes with Re(I) bound via N7 of the NMP; no {N7,P$_\alpha$} macrochelate-type complexes were identified.[17] However, the second phosphate group of monoester diphosphates (MDPs) provides additional binding sites for the *fac*-[Re(CO)$_3$]$^+$ center; thus, different products could result.

Stereochemistry and Nomenclature. The MDPs studied here (Figure 1) have the following characteristics: no asymmetric ribose nor Re(I)-binding base (thiamine diphosphate, TDP), an asymmetric ribose but no Re(I)-binding base (uridine 5′-diphosphate, 5′-UDP), or an asymmetric ribose and a Re(I)-binding base (guanosine 5′-diphosphate, 5′-GDP).

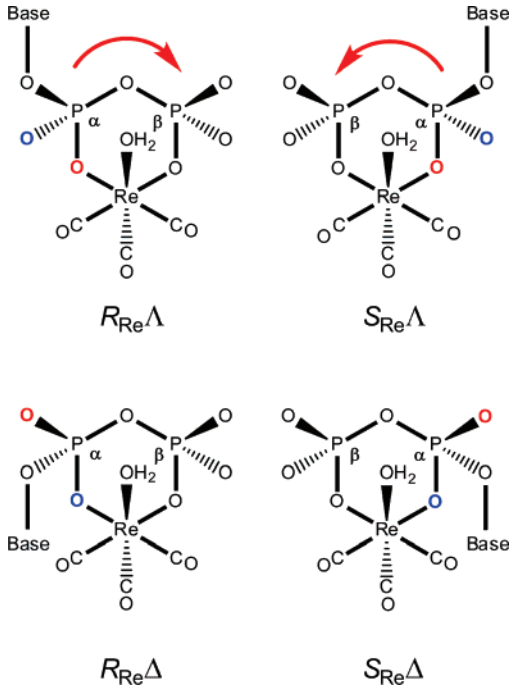

Figure 2. Four possible isomers of *fac*-[Re(CO)$_3$({P$_\alpha$,P$_\beta$}MDP)]$^-$; $R_{Re}\Delta/S_{Re}\Lambda$ and $R_{Re}\Lambda/S_{Re}\Delta$ are mirror image pairs if the attached ester moiety has no chiral groups. Arrows indicate sense of rotation defining chirality at Re(I). The blue O and the red O are the pro-Δ and pro-Λ oxygens in the free nucleotide, respectively.

Although there are potential metal-binding sites on all three base moieties, both N1′ (thiamine, pK_a ∼5) and N3 (uridine, pK_a ∼10) are protonated at pH 3.6, used here; the N7 of guanine (pK_a < 2) is available for binding to Re(I).[4,21] As the complexity of the MDP increases, the number of possible adducts formed by *fac*-[Re(CO)$_3$(H$_2$O)$_3$]$^+$ increases in the order TDP < 5′-UDP < 5′-GDP. Note: in designating the adducts, we omit the 5′- to simplify the designation, but retain the 5′- when referring to the free nucleotide.

Unidentate coordination of an MDP (MDP = TDP, 5′-UDP, 5′-GDP) to *fac*-[Re(CO)$_3$(H$_2$O)$_3$]$^+$ could occur in three possible ways. Coordination via the terminal P$_\beta$ group of an MDP would result in the formation of a single isomer, as the P$_\beta$ group is not prochiral. Unidentate coordination of the prochiral P$_\alpha$ group (although unlikely) would create an asymmetric P$_\alpha$ center and two isomers. The terminal oxygens of the prochiral P$_\alpha$ group are labeled pro-Δ and pro-Λ in Figure 2. Coordination via N7 of 5′-GDP would lead to a single isomer.

Bidentate coordination to *fac*-[Re(CO)$_3$(H$_2$O)$_3$]$^+$ by *both* P$_\alpha$ and P$_\beta$ of an MDP, forming *fac*-[Re(CO)$_3$(H$_2$O)({P$_\alpha$,P$_\beta$}-MDP)]$^-$, creates asymmetric centers at both P$_\alpha$ and Re(I). Up to four diastereomers could exist for the MDP used here. Naming the isomers requires designation of the chirality of these asymmetric centers. First, the asymmetry at P$_\alpha$ depends on which oxygen (pro-Δ or pro-Λ) binds to Re(I) (Figure 2).[5−7] Second, designation of the asymmetry of the Re(I) center is based on the direction of rotation of the MDP around a reference axis defined by a line passing through

(12) Reily, M. D.; Hambley, T. W.; Marzilli, L. G. *J. Am. Chem. Soc.* **1988**, *110*, 2999−3007.
(13) Reily, M. D.; Marzilli, L. G. *J. Am. Chem. Soc.* **1986**, *108*, 8299−8300.
(14) Wong, H. C.; Shinozuka, K.; Natile, G.; Marzilli, L. G. *Inorg. Chim. Acta* **2000**, *297*, 36−46.
(15) Benedetti, M.; Tamasi, G.; Cini, R.; Marzilli, L. G.; Natile, G. *Chem. Eur. J.* **2007**, *13*, 3131−3142.
(16) Natile, G.; Marzilli, L. G. *Coord. Chem. Rev.* **2006**, *250*, 1315−1331.
(17) Adams, K. M.; Marzilli, L. G. *Inorg. Chem.* **2007**, *46*, 4926−4936.
(18) Zobi, F.; Blacque, O.; Schmalle, H. W.; Spingler, B.; Alberto, R. *Inorg. Chem.* **2004**, *43*, 2087−2096.
(19) Zobi, F.; Spingler, B.; Fox, T.; Alberto, R. *Inorg. Chem.* **2003**, *42*, 2818−2820.
(20) Egli, A.; Hegetschweiler, K.; Alberto, R.; Abram, U.; Schibli, R.; Hedinger, R.; Gramlich, V.; Kissner, R.; Schubiger, P. A. *Organometallics* **1997**, *16*, 1833−1840.
(21) Malandrinos, G.; Louloudi, M.; Koukkou, A. J.; Sovago, I.; Drainas, C.; Hadjiliadis, N. *J. Biol. Inorg. Chem.* **2000**, *5*, 218−226.

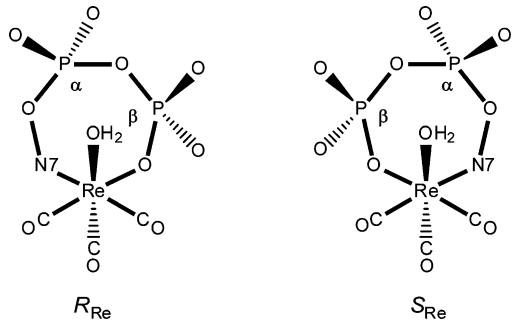

Figure 3. R_{Re} and S_{Re} isomers of *fac*-$[Re(CO)_3(H_2O)(\{N7,P_\beta\}GDP)]^-$. Only these two isomers are possible when P_α is not bound to Re(I). The R_{Re} and S_{Re} isomers are tentatively assigned as ***M*** and ***m***, respectively.

Table 1. Possible Isomers Formed by the Reaction of *fac*-$[Re(CO)_3(H_2O)_3]^+$ with MDPs

complex	diastereomers	mirror pairs	*possible* sets of signals	*observed* sets of signals
$\{P_\alpha,P_\beta\}$TDP	4	2	2	2
$\{P_\alpha,P_\beta\}$UDP	4	0	4	4
$\{N7,P_\alpha,P_\beta\}$GDP	4	0	4	[a]
$\{N7,P_\beta\}$GDP	2	0	2	2

[a] Not observed.

the Re(I) atom perpendicular to the chelate ring (assumed to be planar as shown in Figure 2) and passing through the CO (away from the viewer).[5−7] The asymmetry at Re(I) is then designated as R_{Re} and S_{Re} for clockwise and counterclockwise rotation, respectively (Figure 2). Although we adhere to the naming protocol described here, we should note that application of the *R*,*S* system (according to Cahn−Ingold−Prelog priority rules) to other metal−chelate complexes can lead to reversals of the letter designation.[5] In *fac*-$[Re(CO)_3(H_2O)(\{P_\alpha,P_\beta\}MDP)]^-$ adducts, the four possible diastereomers constitute two enantiomeric pairs (two sets of NMR signals, $R_{Re}\Delta/S_{Re}\Lambda$ and $R_{Re}\Lambda/S_{Re}\Delta$) for TDP but four NMR-distinct isomers for 5′-UDP ($R_{Re}\Delta$, $R_{Re}\Lambda$, $S_{Re}\Delta$, $S_{Re}\Lambda$, Figure 2). Were 5′-GDP to bind in this manner, there would again be four NMR-distinct diastereomers. However, we did not detect clear evidence for such a species because 5′-GDP binds via N7 in all major species we identified; Re(I) coordination via N7 of 5′-GDP presents different possibilities for adduct formation. Bidentate coordination through N7 *and* P_β of 5′-GDP creates only one asymmetric center (at Re(I)). If the resulting pair of diastereomers (R_{Re} and S_{Re}) of *fac*-$[Re(CO)_3(H_2O)(\{N7,P_\beta\}GDP)]^-$ (Figure 3) is conformationally dynamic, only two sets of NMR signals are expected. Tridentate coordination of N7, P_α, *and* P_β of 5′-GDP, to form the *fac*-$[Re(CO)_3\{N7,P_\alpha,P_\beta\}GDP)]^-$ adduct, would result in four NMR-distinct diastereomers because this adduct contains both Re(I) and P_α asymmetric centers. The number of possible adducts and NMR-observable distinct sets of signals are summarized in Table 1.

Experimental Section

Materials and Sample Preparation. Stock solutions (10 and 50 mM) of *fac*-$[Re(CO)_3(H_2O)_3]$OTf in H_2O were prepared by published procedures and maintained at pH ∼1.8.[22] 5′-GDP, 5′-UDP (disodium salts), TDP, sodium pyrophosphate (PP), and D_2O (99.9%) (Sigma-Aldrich) were used as received.

A typical preparation of samples for 1D NMR spectroscopy involved treatment of an appropriate amount of MDP in 0.3 mL of H_2O with 0.4 mL of an ∼10 mM stock solution of *fac*-$[Re(CO)_3(H_2O)_3]$OTf; a small amount (0.1 mL) of D_2O was added to establish a lock signal. For 2D NMR spectroscopy, samples were prepared by removing H_2O from an aqueous 0.4 mL aliquot of a ∼50 mM stock solution of *fac*-$[Re(CO)_3(H_2O)_3]$OTf and adding 0.4 mL of D_2O; then, the appropriate amount of MDP (in 0.4 mL D_2O) was added. The pH (uncorrected) of the samples in NMR tubes was maintained at ∼3.6 by the addition of dilute HCl and NaOH (in H_2O) or DCl and NaOD (in D_2O) stock solutions, as required. The pH of each sample was adjusted before the acquisition of each NMR spectrum. Because spectra were acquired at frequent intervals relative to the ∼1 day half-life of each reaction, the reactions proceeded at a pH close to 3.6. At early stages of the reactions, the pH changes were larger, and generally the pH dropped. However, our focus was on the products, not on the reaction rates of product formation.

NMR Spectroscopy. All NMR spectra were obtained on a Varian INOVA500 spectrometer (500.1 MHz) equipped with a variable-temperature probe that was equilibrated at 25 °C unless otherwise indicated. A 1 s presaturation pulse was used to reduce the HOD peak in 1D ^1H NMR spectra, and the residual HOD signal was used to reference the spectrum. Each FID was accumulated for 32 transients, each containing 32K data points. Before Fourier transformation, an exponential apodization window function with a 0.2 Hz line-broadening was applied. 1D proton-decoupled ^{31}P NMR spectra ($\{^1H\}$-^{31}P) were referenced to external trimethyl phosphate (TMP); each FID was accumulated for 128 transients, each containing 8K data points. Before Fourier transformation, an exponential apodization window function with a 0.5 Hz line-broadening was applied.

In general, 32 scans per block (512 blocks) were collected in $^1H-^1H$ rotating frame nuclear Overhauser effect spectroscopy (ROESY) experiments conducted by using a spectral width of ∼6000 Hz in both dimensions and a mixing time of 500 ms at 25 and 32 °C. Proton-decoupled $^{31}P-^{31}P$ nuclear Overhauser effect spectroscopy (NOESY) exchange experiments were conducted by using 32 scans per block (422 blocks) and a spectral width of ∼5000 Hz in both dimensions and a mixing time of 500 ms at 32 °C. Proton-decoupled $^{31}P-^{31}P$ correlation spectroscopy (COSY) experiments containing 32 scans per block (734 blocks) were conducted by using a spectral width of ∼4400 Hz in both dimensions and a COSY-45 pulse sequence to aid in visualizing close coupling patterns. All NMR data were processed with VnmrJ (Varian) software.

Computational Methods. All models were constructed on a PC equipped with the Hyperchem 7.5[23] molecular modeling package, and all computations were performed using AMBER99 force field parameters and methods described previously.[24] Four models (two R_{Re} and two S_{Re} models) of *fac*-$[Re(CO)_3(H_2O)(\{N7,P_\beta\}GDP)]^-$ were built by using information obtained through NMR studies and derived from the X-ray crystal structure of *fac*-$[Re(CO)_3(H_2O)(9\text{-MeG})_2]^+$.[18] The Re−N7 distance in all four models was constrained to ∼2.2 Å. The H2′−C2′−C1′−H1′ angle of one R_{Re} and one S_{Re} model was constrained to 67° (equal to a $^3J_{H1'-H2'}$ value of 1 Hz), and the H2′−C2′−C1′−H1′ angle of the other R_{Re} and S_{Re} models was constrained to 41° (equal to a $^3J_{H1'-H2'}$ value of 4.5 Hz). The

(22) He, H.; Lipowska, M.; Xu, X.; Taylor, A. T.; Carlone, M.; Marzilli, L. G. *Inorg. Chem.* **2005**, *44*, 5437−5446.
(23) *HyperChem, Version 7.5*; Hypercube, Inc.: Gainesville, FL.
(24) He, H.; Lipowska, M.; Christoforou, A. M.; Marzilli, L. G.; Taylor, A. T. *Nucl. Med. Biol.* **2007**, *34*, 709−716.

Table 2. ^{1}H and ^{31}P NMR Chemical Shifts (ppm), Coupling Constants (Hz) of TDP, 5′-UDP, PP, and Complexes Formed with *fac*-[Re(CO)$_3$(H$_2$O)$_3$]$^+$ [a]

complex	δ ^{1}H		δ ^{31}P	
PP	–	–	−13.8	
fac-[Re(CO)$_3$(H$_2$O)(PP)]$^-$	–	–	−6.6	
	H2	H6′	P$_\alpha$ ($J_{\alpha\beta}$)	P$_\beta$
TDP	9.62	7.88	−14.7 (22.3)	−14.0
M pair	9.71	7.79	−9.0 (19.8)	−5.0
m pair	9.67	7.77	−8.4 (19.6)	−4.9
	H6	H1′ ($^3J_{H1'-H2'}$)	P$_\alpha$ ($J_{\alpha\beta}$)	P$_\beta$ ($J_{\beta\alpha}$)
5′-UDP	7.94[b]	5.98 (4.5)[c]	−14.4 (20.2)	−13.8 (20.3)
M$_1$	7.98[b]	5.95[c]	−9.2 (20.6)	−5.4 (20.4)
m$_1$	7.88[b]	5.95[c]	−8.8 (19.8)	−5.6 (20.7)
M$_2$	7.87[b]	5.95[c]	−8.5 (19.8)	−5.7 (20.2)
m$_2$	7.86[b]	5.95[c]	−8.5 (19.8)	−5.5 (20.2)

[a] 25 mM, r = 1:1, pH 3.6. [b] $^3J_{H5-H6}$ = 8.1 Hz. [c] H1′ signals overlap with H5 signals.

H8 proton was oriented close in space to H2′ and H3′ in all four models, as the NOE data (see above) confirms this close proximity for all adducts formed. The models were geometrically minimized using Polak−Ribiere conjugate gradient minimization, which was terminated upon reaching an rms gradient of 0.01 kcal/Å·mol.

Results and Discussion

Shift changes of the ^{1}H and ^{31}P NMR signals of the MDP upon coordination are informative. In general, ^{1}H and ^{31}P NMR signals arising from atoms close to the metal binding site will shift downfield upon coordination because of an inductive effect of the metal center. Because deprotonation of *fac*-[Re(CO)$_3$(H$_2$O)$_3$]$^+$ begins around pH 4 and causes oligomerization, we conducted most studies at pH 3.6 as in previous work.[17,20] In addition, 5′-GDP is protonated at N7 to a very limited extent at pH 3.6 (see NMR shift data in the Supporting Information), thereby allowing metal coordination; also, the low pH assures no significant deprotonation of N1H, thereby precluding metal binding at N1. Coordination of Re(I) at N7 of 5′-GMP causes a ∼0.4 ppm downfield shift of the H8 signal and a slight upfield shift (∼0.3 ppm) of the P$_\alpha$ signal, while coordination of one Re(I) metal center at N7 and another at P$_\alpha$ of the same 5′-GMP leads to a ∼0.4 ppm downfield shift of the H8 signal but a larger ∼4 ppm downfield shift of the P$_\alpha$ signal.[17] At pH ∼3.6, the P$_\beta$ group of the free MDP is protonated and the phosphate chain carries two negative charges (Figure 1).

Throughout this section, concentrations will be denoted as (_ _ mM, r = __:__), in which the *fac*-[Re(CO)$_3$(H$_2$O)$_3$]$^+$ concentration is stated and r is the ratio of the cation to added phosphate ligand. This notation designates both the starting ligand concentration and its ratio to the starting *fac*-[Re(CO)$_3$(H$_2$O)$_3$]$^+$ concentration.

As a first step, we employed diprotonated pyrophosphate (PP^{2-}) to assess the effects of chelate ring formation on ^{31}P NMR shifts at pH ∼3.6. A single product ^{31}P NMR signal, shifted ∼7 ppm downfield from the ^{31}P NMR signal of free PP^{2-} (Table 2), was observed 1 day after mixing *fac*-[Re(CO)$_3$(H$_2$O)$_3$]$^+$ and PP^{2-} (25 mM, r = 1:1 and 1:2). At equilibrium (no changes from 3 to 6 days), ∼60% of the PP^{2-} had reacted, indicating incomplete product formation. The appearance of one signal indicates that *fac*-[Re(CO)$_3$(H$_2$O)(PP)]$^-$, in which both phosphate groups chelate Re(I), is the reaction product.

Overview of Products Formed by *fac*-[Re(CO)$_3$(H$_2$O)$_3$]$^+$ and MDPs. In describing the results for MDP binding to *fac*-[Re(CO)$_3$(H$_2$O)$_3$]$^+$, we state the nature of the adducts formed before presenting all the ^{1}H and ^{31}P NMR spectral evidence and the reasoning for adduct designations. We should note that no evidence was found for the formation of significant amounts of either unidentate adducts (bound through only one phosphate oxygen) or 1:2 adducts for any MDP, even in r = 1:2 reaction mixtures.

TDP Reaction Products. TDP formed a 1:1 adduct, *fac*-[Re(CO)$_3$(H$_2$O)({P$_\alpha$,P$_\beta$}TDP)]$^-$, for which four diastereomers are possible (Figure 2). Because these are two mirror-image pairs ($R_{Re}\Delta/S_{Re}\Lambda$ and $R_{Re}\Lambda/S_{Re}\Delta$), only two sets of ^{1}H and ^{31}P NMR signals for bound TDP were observed. The more intense set is labeled ***M*** for the major mirror-image pair, and the other set is labeled ***m*** for the minor mirror-image pair.

Although the 5a and 5b multiplets are for TDP protons close to the metal-binding P$_\alpha$ phosphate group (Figure 1), these multiplets have chemical shifts very close to that of residual HOD. Thus, the H2 and H6′ singlets, although for protons remote from the metal-binding site, are also used to provide information about the adducts formed. Approximately 1 day after *fac*-[Re(CO)$_3$(H$_2$O)$_3$]$^+$ and TDP (25 mM, r = 1:1) were mixed, the NMR spectrum showed two new H2 and two new H6′ singlets, shifted slightly downfield and slightly upfield, respectively, from the corresponding H2 and H6′ signals of free TDP (Table 2). Although partially obscured by the residual HOD peak, two sets of 5b multiplets (shifted downfield from the 5b multiplet of free TDP) were observed. At equilibrium (no changes from 3 to 6 days), the ratio of ***M*** pair/***m*** pair was 2:1 and only ∼35% of the TDP had reacted, indicating incomplete product formation.

The {^{1}H}-^{31}P NMR spectrum of the (25 mM, r = 1:1) reaction mixture revealed two P$_\alpha$ doublets at ca. −8.7 ppm and two P$_\beta$ doublets at ca. −5.0 ppm, shifted ∼6 and ∼9 ppm downfield from the respective free TDP signals (Figure 4). The P$_\alpha$ vs P$_\beta$ assignments were confirmed with a proton-coupled ^{31}P NMR spectrum. A proton-decoupled ^{31}P−^{31}P COSY experiment (25 mM, r = 1:1) showed coupling between doublets at −9.0 (P$_\alpha$) and −5.0 ppm (P$_\beta$) for the

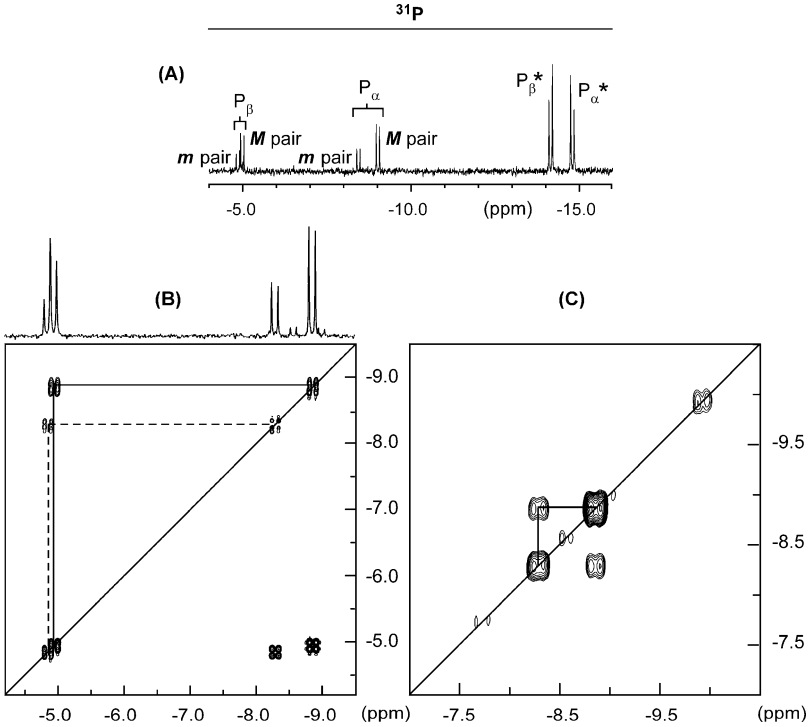

Figure 4. ^{31}P NMR (A), ^{31}P−^{31}P COSY **(B)**, and ^{31}P−^{31}P NOESY **(C)** spectra of an equilibrium mixture of *fac*-[Re(CO)$_3$(H$_2$O)$_3$]$^+$ (25 mM, r = 1:1) and TDP at pH 3.6. Asterisk labels indicate peaks arising from free TDP.

major pair (***M*** pair), and doublets at −8.4 (P_α) and −4.9 ppm (P_β) for the minor pair (***m*** pair, Figure 4). In addition, a ^{31}P−^{31}P NOESY spectrum showed exchange between the two P_α doublets and between the P_β doublets, indicating that interconversion of the isomers does occur, but in the slow-exchange regime of the NMR time scale (see below).

The P_β signals of ***M*** pair and ***m*** pair shifted ∼4 ppm downfield between pH 1.5 and 3.5 during an NMR-monitored titration from pH 1.5 to 6.5, leading to a pK_a estimate of ∼2.5 for P_β of both the ***M*** and ***m*** pairs. The low value of the estimated P_β pK_a is likely due to the presence of a proton on N1′.

5′-UDP Reaction Products. 5′-UDP formed a 1:1 adduct, *fac*-[Re(CO)$_3$(H$_2$O)({P$_\alpha$,P$_\beta$}UDP)]$^-$, exhibiting ^{1}H and ^{31}P NMR signals of four diastereomers. (The Re/5′-UDP 1:1 ratio in the adduct was confirmed in the mixed-nucleotide experiment described below.) Because the H5 and H1′ signals overlap, only the H6 signals are informative. ^{1}H NMR spectra of *fac*-[Re(CO)$_3$(H$_2$O)$_3$]$^+$ treated with 5′-UDP (25 mM, r = 1:1) showed after ∼1 day one large H6 doublet (***M$_1$***) and three smaller H6 doublets (***M$_2$***, ***m$_1$***, ***m$_2$***), shifted slightly *downfield* and slightly *upfield*, respectively, from the H6 doublet of free 5′-UDP (Figure 5, Table 2). The small size of the shifts indicates no base binding. At equilibrium (no changes from 3 to 6 days), ∼40% of the 5′-UDP had reacted (17% large H6 and 23% other three H6's combined), indicating that 5′-UDP product formation is about as favorable as TDP product formation at r = 1:1. This finding is consistent with the absence of base binding for both MDPs.

The {^{1}H}-^{31}P NMR spectrum of the (25 mM, r = 1:1) reaction mixture revealed three well-separated P_α doublets at ca. −8.8 ppm and four overlapping P_β doublets at ca. −5.6 ppm, shifted ∼6 and ∼8 ppm downfield from the respective free 5′-UDP signals (Figure 5). The P_α doublets are assigned as follows. Most upfield, ***M$_1$***; intermediate, ***m$_1$***; the most downfield, both ***M$_2$*** and ***m$_2$***. The P_α vs P_β assignments were confirmed with a proton-coupled ^{31}P NMR spectrum. A proton-decoupled ^{31}P−^{31}P COSY experiment (25 mM, r = 1:1) revealed the ***M$_1$***/***M$_2$*** and ***m$_1$***/***m$_2$*** connectivities between the P_α and P_β signals (Figure 5). The ^{31}P−^{31}P NOESY spectrum showed exchange between the downfield overlapped ***M$_2$*** and ***m$_2$*** P_α doublet and the two ***M$_1$*** and ***m$_1$*** P_α doublets, but no exchange between the ***M$_1$*** and ***m$_1$*** P_α doublets was detected (see below).

Mixed-Nucleotide Experiment. To investigate the Re/nucleotide ratio of the products, we treated *fac*-[Re(CO)$_3$(H$_2$O)$_3$]$^+$ with a mixture of TDP and 5′-UDP (25 mM, r = 1:0.5:0.5 and 1:1:1). If the adducts identified above as 1:1 adducts were in fact 1:2 adducts or 2:2 adducts, etc., new product NMR signals for mixed TDP/5′-UDP adducts would be observed. At equilibrium, no unidentified NMR signals were observed, the ratio of the four product 5′-UDP H6 signals did not change, and the total amount of reaction was comparable to that found in the (25 mM, r = 1:1) experiment, thus confirming that only one MDP is bound per Re(I). In addition, monitoring of a *fac*-[Re(CO)$_3$(H$_2$O)$_3$]$^+$ plus 5′-UDP (25 mM, r = 1:1) equilibrated reaction mixture after addition of 3 equiv of TDP confirmed that 5′-UDP dissociation was very slow ($t_{1/2} \approx$ 24 h). A reviewer commented that this type of observation would support the suggested mechanism for the isomerizations described below. We postulate below that P_β does not dissociate during the isomerization process.

5′-GDP Reaction Products. 5′-GDP formed mainly three 1:1 adducts: *fac*-[Re(CO)$_3$(H$_2$O)$_2$({N7}GDP)]$^-$ and two

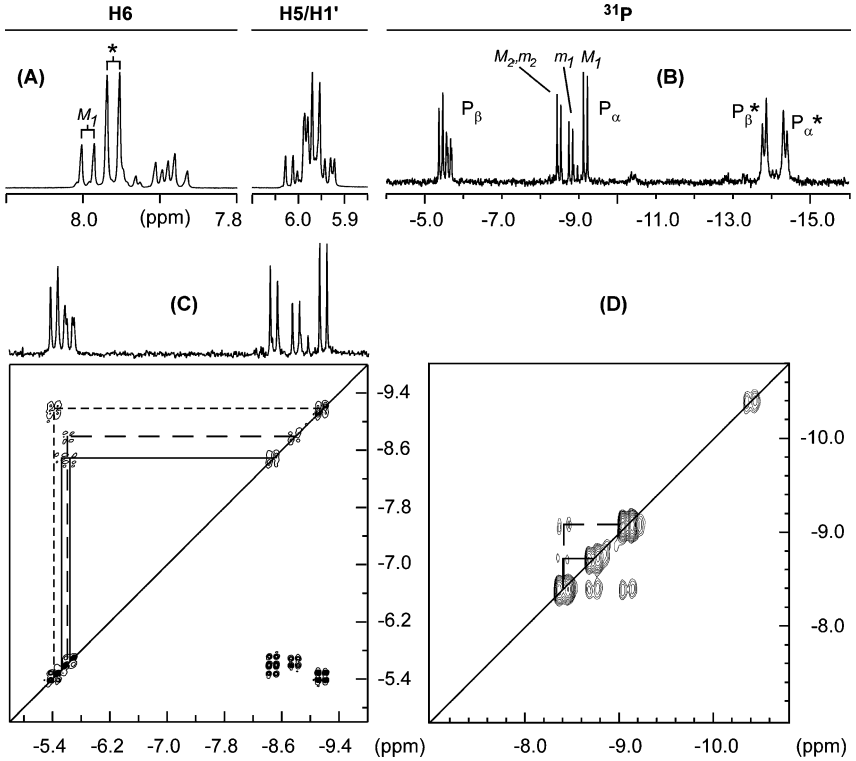

Figure 5. ^{1}H NMR **(A)**, ^{31}P NMR **(B)**, ^{31}P−^{31}P COSY **(**C), and ^{31}P−^{31}P NOESY **(D)** spectra of an equilibrium mixture of *fac*-[Re(CO)$_3$(H$_2$O)$_3$]$^+$ (25 mM, r = 1:1) and 5′-UDP at pH 3.6. Asterisk labels indicate peaks arising from free 5′-UDP.

isomers of *fac*-[Re(CO)$_3$(H$_2$O)({N7,P$_\beta$}GDP)]$^-$ (***M*** and ***m***). Only one set of NMR signals was observed for each species. The most informative ^{1}H NMR signals of 5′-GDP are H8 (on the base) and H1′ (on the ribose); extensive studies with metal−**G** (**G** = a guanine N9 derivative) complexes indicate that, upon coordination of **G** via N7, the **G** H8 singlet shifts downfield.[25] Because of the inductive effect of the metal center, the H1′ doublet shifts downfield slightly upon formation of a 1:1 adduct. An {N7,P$_\alpha$} macrochelate, in which the 5′-nucleotide is coordinated via both N7 and P$_\alpha$, has an H1′ signal that appears to be a singlet.[12,13,26] The coupling constant, $^3J_{H1'-H2'}$, is dependent upon the mole fractions of N and S sugar pucker present in dynamic equilibrium; typical free MDPs have $^3J_{H1'-H2'}$ values of ∼6 Hz and %S ≈ 10 × $^3J_{H1'-H2'}$ (corresponding to ∼60% S pucker).[27] As the mole fraction of N sugar increases, the $^3J_{H1'-H2'}$ value decreases, approaching 0 Hz near 100% N.[27] However, an {N7,P$_\alpha$} macrochelate is rare, occurring for 5′- but not for 3′-nucleotides.[13,28,29]

Upon treatment of *fac*-[Re(CO)$_3$(H$_2$O)$_3$]$^+$ with 5′-GDP (25 mM, r = 1:1), three new H8 NMR singlets and two new H1′ signals were observed immediately after mixing (Figure 6, Table 3). The two most downfield product H8 signals (8.79 and 8.67 ppm, ***M*** and ***m***, respectively) integrate as 1:0.86, respectively, at 1 day after mixing and at equilibrium (no changes from 3 to 6 days). The smallest, least downfield product H8 singlet (8.49 ppm) decreased in intensity with time relative to the two larger H8 product signals; at equilibrium, the ***M***/8.49 ppm signal ratio was 1:0.17. A number of other small H8 signals are unambiguously due to traces of free 5′-GMP present in the starting 5′-GDP and the resulting *fac*-[Re(CO)$_3$(H$_2$O)$_2$(5′-GMP)] adduct.[17] The finding that at equilibrium 83% of the 5′-GDP has reacted indicates that 5′-GDP binds more strongly than 5′-UDP or TDP.

The {^{1}H}-^{31}P NMR spectrum of the (25 mM, r = 1:1) reaction mixture revealed signals attributable to at least three products. From proton-coupled ^{31}P NMR spectroscopy, the two large doublets at −14.3 (***M***) and −12.7 (***m***) ppm are P$_\alpha$ signals, while the two overlapped doublets at −10.8 ppm are P$_\beta$ signals. A proton-decoupled ^{31}P−^{31}P COSY experiment (25 mM, r = 1:1) showed coupling between P$_\alpha$ and P$_\beta$ for the products (Figure 6). A ^{31}P−^{31}P NOESY spectrum showed exchange between the P$_\alpha$ doublets of ***M*** and ***m***; no exchange was detected between the P$_\beta$ signals of ***M*** and ***m***, as these signals overlap (Figure 7). These ^{31}P NMR results support the ^{1}H NMR evidence indicating the presence of *two* isomers of *fac*-[Re(CO)$_3$(H$_2$O)({N7,P$_\beta$}GDP)]$^-$ (***M*** and ***m***). The results show that P$_\beta$ is directly coordinated to Re(I) and that P$_\alpha$ *is not* directly coordinated to Re(I) in both ***M*** and ***m***. The minor third product, *fac*-[Re(CO)$_3$(H$_2$O)$_2$({N7}GDP)]$^-$, was characterized by small P$_\alpha$ and P$_\beta$ doublets that were slightly shifted (−14.6 and −13.7 ppm, respectively) from the corresponding signals of free 5′-GDP.

(25) Ano, S. O.; Kuklenyik, Z.; Marzilli, L. G. In *Cisplatin: Chemistry and Biochemistry of a Leading Anticancer Drug*; Lippert, B., Ed.; Wiley-VCH: Weinheim, 1999; pp 247−291.
(26) Girault, J.-P.; Chottard, G.; Lallemand, J.-Y.; Chottard, J.-C. *Biochemistry* **1982**, *21*, 1352−1356.
(27) Altona, C.; Sundaralingam, M. *J. Am. Chem. Soc.* **1973**, *95*, 2333−2344.
(28) Kuo, L. Y.; Kanatzidis, M. G.; Marks, T. J. *J. Am. Chem. Soc.* **1987**, *109*, 7207−7209.
(29) Torres, L. M.; Marzilli, L. G. *J. Am. Chem. Soc.* **1991**, *113*, 4678−4679.

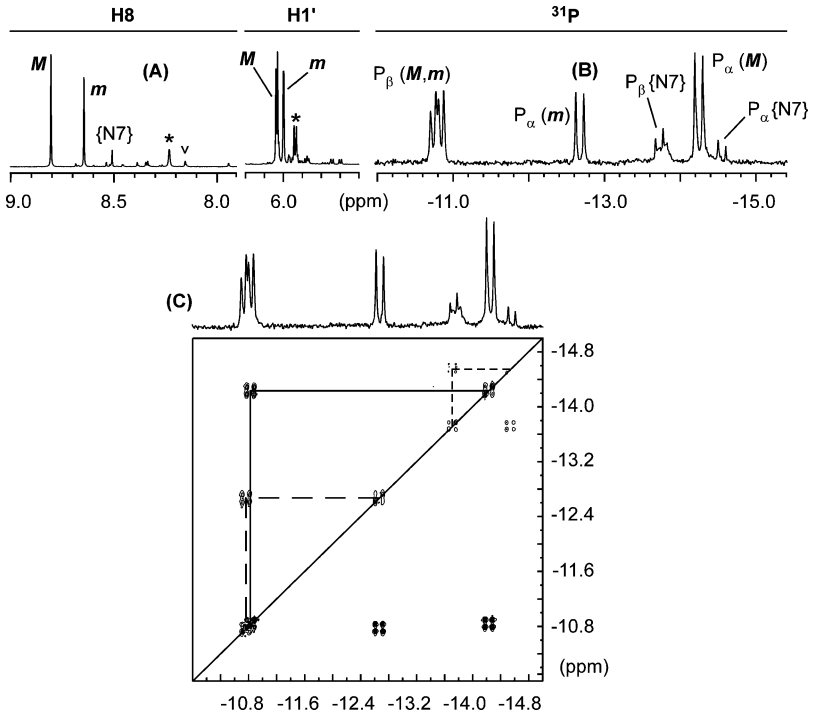

Figure 6. ^{1}H NMR **(A)**, ^{31}P NMR **(B)** and ^{31}P−^{31}P COSY **(C)** spectra of an equilibrium mixture of *fac*-[Re(CO)$_3$(H$_2$O)$_3$]$^+$ (25 mM, r = 1:1) and 5′-GDP at pH 3.6. Asterisk labels indicate peaks arising from free 5′-GDP.

Table 3. ^{1}H and ^{31}P NMR Chemical Shifts (ppm), Coupling Constants (Hz) of 5′-GDP and Complexes Formed with *fac*-[Re(CO)$_3$(H$_2$O)$_3$]$^+$ [a]

	δ ^{1}H		δ ^{31}P	
complex	H8	H1′ ($^{3}J_{H1'-H2'}$)	P$_\alpha$ ($J_{\alpha\beta}$)	P$_\beta$
5′-GDP	8.21	5.92 (6.0)	−14.6 (21.5)	−13.8
fac-[Re(CO)$_3$(H$_2$O)$_2$({N7}GDP)]$^-$	8.49	6.03[b]	−14.6 (19.7)	−13.7
M	8.79	6.03 (4.5)	−14.3 (21.5)	−10.8
m	8.67	6.00 (1.0)	−12.7 (21.5)	−10.8

[a] 25 mM, r = 1:1, pH 3.6. [b] Assigned by a ^{1}H−^{1}H ROESY experiment.

All free 5′-GDP was consumed in an experiment with an excess of Re(I) (25 mM, r = 1:0.5). Five hours after mixing, we observed at least three new H8 signals, shifted ca. 0.4 ppm downfield from the H8 signal of free 5′-GDP, in addition to the H8 signals of ***M***, ***m***, and *fac*-[Re(CO)$_3$(H$_2$O)$_2$-({N7}GDP)]$^-$. ***M***, ***m***, and *fac*-[Re(CO)$_3$(H$_2$O)$_2$({N7}GDP)]$^-$ accounted for 78% of the reacted 5′-GDP, while the three new H8 signals accounted for 22% of the reacted 5′-GDP. At r = 1:0.5, the ***m*** H8 signal appears to be larger than the ***M*** H8 signal, but this result is likely due to overlap of the ***m*** H8 signal with another new H8 signal. The {^{1}H}-^{31}P NMR spectrum showed three new P$_\alpha$ doublets between −7.5 and −8.5 ppm; these shifts are within ∼0.5 ppm of the P$_\alpha$ doublets of the TDP and 5′-UDP adducts (ca. −8.5 ppm for both). Likewise, the shifts of the two sets of two new P$_\beta$ doublets at ca. −4 and −4.5 ppm are within ∼1 ppm of those for the P$_\beta$ doublets of the TDP and 5′-UDP adducts (−5 and −5.5 ppm, respectively). Thus, these results indicate that the new products all have N7, P$_\alpha$, and P$_\beta$ of 5′-GDP bound to Re(I). An increase in the amount of these new products upon addition of an excess of *fac*-[Re(CO)$_3$(H$_2$O)$_3$]$^+$ indicates that more than one Re(I) is bound per 5′-GDP. Therefore, the new products are undoubtedly dinuclear species with N7 bound to one Re(I) moiety and P$_\alpha$ and P$_\beta$ chelating a second Re(I) moiety.

Further Considerations. Our evidence demonstrates that all three products of the r = 1:1 reaction are N7-bound 1:1 adducts, *fac*-[Re(CO)$_3$(H$_2$O)$_x$(GDP)]$^-$ (x = 1 or 2). There are four types of evidence for N7 binding: First, the downfield shift changes of the H8 singlets (∼0.5 ppm) and the H1′ NMR signals (∼0.1 ppm) of these products relative to free 5′-GDP are consistent with N7-bound adducts (Table 2).[17] Second, the three H8 singlets were insensitive to changing the pH from 3.6 to 1.5 (Supporting Information).[17] Third, $^{3}J_{H1'-H2'}$ decreased from ∼5.6 Hz (free 5′-GDP) to ∼4.5 and ∼1 Hz, a feature consistent with metal coordination at N7 (Table 2).[17] Furthermore, $^{3}J_{H1'-H2'} \approx$ 1 Hz is indicative of an N7-coordinated, macrochelate-type structure having a highly N-puckered ribose.[27] Fourth, titration of a solution of Mn^{2+} ion (1 mM) into an equilibrated solution of *fac*-[Re(CO)$_3$(H$_2$O)$_3$]$^+$ and 5′-GDP (5 mM, r = 1:1) confirmed that N7 was bound to Re(I) in all three products, as none of the three H8 NMR signals of bound 5′-GDP broadened significantly at 5 μM Mn^{2+} ion, a concentration at which the H8 signal of free 5′-GDP became broadened to the point of disappearance (Supporting Information). Two types of evidence demonstrate that all products have one Re(I) per 5′-GDP: First, all three H8 signals have different integrals (Supporting Information). Two of the three H8 signals would integrate equally if they were due to a bis adduct, in which both nucleotides are coordinated to the same Re(I) center.[17] Second, addition of a second equivalent of 5′-GDP to a previously equilibrated sample (25 mM, r = 1:1) such that r = 1:2 resulted in 57% of the 5′-GDP remaining unbound. Taken together, the above findings leave no doubt that all three products contain one N7-bound 5′-GDP.

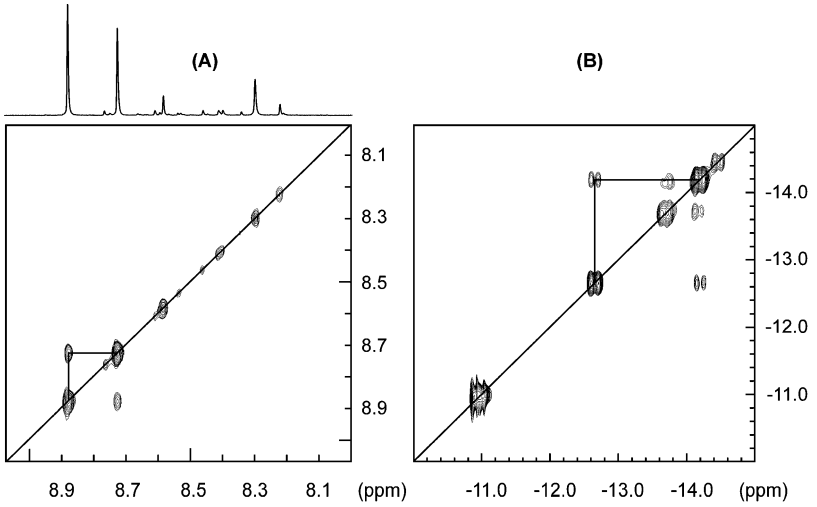

Figure 7. ^{1}H−^{1}H ROESY (A) and ^{31}P−^{31}P NOESY (B) spectra of an equilibrium mixture of *fac*-[Re(CO)$_3$(H$_2$O)$_3$]$^+$ (25 mM, r = 1:1) and 5′-GDP at pH 3.6.

Table 4. Ribose ^{1}H NMR Chemical Shifts (ppm) of 5′-GDP and Complexes Formed with *fac*-[Re(CO)$_3$(H$_2$O)$_3$]$^+$ [a]

	δ ^{1}H			
complex	H2′	H3′	H4′	H5′/H5″
5′-GDP	4.70	4.54	4.30	4.18/4.18
fac-[Re(CO)$_3$(H$_2$O)$_2$({N7}GDP)]$^-$	4.63	4.53	4.36	[b]
M	4.59	4.48	4.34	4.35/4.15
m	4.35	4.43	4.29	4.19/4.13

[a] 25 mM, r = 1:1, pH 3.6. [b] Not observed.

The ribose ^{1}H NMR signals of the *fac*-[Re(CO)$_3$(H$_2$O)({N7,P$_\beta$}GDP)]$^-$ isomers were assigned by using ^{1}H−^{1}H COSY and ^{1}H−^{13}C HMQC experiments (Table 4). The H1′ signals at 6.03 and 6.00 ppm belong to ***M*** and ***m***, respectively. $^3J_{H1'-H2'}$ values of ∼4.5 (***M***) and ∼1 (***m***) Hz correspond to ∼55% and ∼90% N pucker, respectively. Most notably, the H2′ NMR signal of ***m*** is shifted *upfield* (∼0.3 ppm) relative to the H2′ NMR signals of ***M*** or *fac*-[Re(CO)$_3$(H$_2$O)$_2$({N7}GDP)]$^-$. Previous studies have shown that the H2′ NMR signal of *cis*-[Pt(NH$_2$CH$_3$)$_2$({N7,P$_\alpha$}5′-IMP)] is shifted significantly *downfield* (0.4 ppm) relative to the H2′ NMR signals of *cis*-[Pt(NH$_2$CH$_3$)$_2$({N7}5′-IMP)] or free 5′-IMP; in this adduct, the sugar is N, the base is anti, and the anisotropic downfield shift of H2′ is likely due to the placement of H2′ in the plane of the pyrimidine ring near N3.[12,13] Conversely, an *upfield* shift of H2′ (0.08 ppm) is seen for N, high anti *cis*-[Pt(ND$_2$CH$_3$)$_2$({N7,P$_\gamma$}5′-ITP)]; the upfield shift of H2′ is likely caused by anisotropy.[12,13] Therefore, these results indicate that in ***m***, the sugar is N, the base is high anti, and the H2′ proton is *not* located near N3 of the base pyrimidine ring.

The syn or anti conformation of bound 5′-GDP in the products was evaluated by using the intensities of the H8−H1′ and H8−H2′ NOE cross-peaks in a ^{1}H−^{1}H ROESY experiment (25 mM, r = 1:1). Weak H8−H1′ and strong H8−H2′ NOE cross-peaks indicate an anti conformation of 5′-GDP, while the reverse is found for 5′-GDP with a syn conformation. The H8−H1′ NOE cross-peaks of ***M***, ***m***, and *fac*-[Re(CO)$_3$(H$_2$O)$_2$({N7}GDP)]$^-$ were weak compared to the H8−H2′ NOE cross-peaks, indicating that the nucleotides in all adducts are in the anti conformation. Also apparent in the ROESY spectrum were ***M***−***m*** H8−H8 EXSY cross-peaks (Figure 7), consistent with the ^{31}P EXSY data, indicating ***M***-to-***m*** interchange.

pH Study of *fac*-[Re(CO)$_3$(H$_2$O)({N7,P$_\beta$}GDP)]$^-$ Isomers. In an effort to identify differences between the two *fac*-[Re(CO)$_3$(H$_2$O)({N7,P$_\beta$}GDP)]$^-$ isomers, we carried out an NMR-monitored titration from pH ∼1.5 to 6.5 in 1-unit steps. The H8 NMR signals of the two *fac*-[Re(CO)$_3$(H$_2$O)({N7,P$_\beta$}GDP)]$^-$ isomers shifted downfield ∼0.2 ppm between pH 3.5 and 5.5; this small downfield shift is most likely a result of deprotonation of the P$_\beta$ group (Supporting Information). In addition, the H8 signal of *fac*-[Re(CO)$_3$(H$_2$O)$_2$({N7}GDP)]$^-$ disappeared around pH 4.5, indicating that this species is not stable at higher pH, converting to the macrochelate isomers. Previous work has shown that 1:1 complexes containing 5′-GMP bound to Re(I) via N7 only are unstable above pH 4.[17] The P$_\alpha$ signals of ***M*** and ***m*** are affected similarly by P$_\beta$ deprotonation, shifting downfield slightly (∼0.6 ppm). The P$_\beta$ signals of ***M*** and ***m*** shifted downfield ∼5 ppm between pH 3.5 and 5.5, indicating that the pK_a of this group has been lowered by ∼2 pH units compared to free 5′-GDP (pK_a ∼6.5, Supporting Information). The similar behavior of the ^{31}P NMR signals over the pH range studied provides additional evidence that ***M*** and ***m*** have closely related structures, as expected if they differ mainly in the chirality at the Re(I) metal center (R_{Re} and S_{Re}, see above).

Mn^{2+} Relaxation NMR Titrations of *fac*-[Re(CO)$_3$(H$_2$O)({N7,P$_\beta$}GDP)]$^-$ Isomers. To investigate the possible differences between the two *fac*-[Re(CO)$_3$(H$_2$O)({N7,P$_\beta$}GDP)]$^-$ isomers, Mn^{2+} ion was used to assess the environment surrounding the H8 proton of each isomer. For example, the H8 NMR signal will broaden upon addition of Mn^{2+} ion if uncoordinated phosphate groups reside near the H8 proton. The magnitude of this line-broadening is slight compared to that observed when N7 is not bound to Re(I), allowing the two phenomena to be distinguished (see above). At increasing concentrations of Mn^{2+} ion, the line width of the H8 NMR

Table 5. Characteristics of Selected Pt(II) and Re(I) Nucleotide Complexes

complex	P (deg)	χ (deg)	N/S	syn/anti
cis-[Pt(NH$_3$)$_2$({N7,P$_\gamma$}5′-GTP)][a]	346	−26.5	N	syn
cis -[Pt(NH$_3$)$_2$({N7,P$_\beta$}5′-GTP)][a]	332	−60.1	N	borderline syn/high anti
cis -[Pt(NH$_3$)$_2$({N7,P$_\alpha$}5′-GTP)][a]	327	−81.5	N	high anti
fac-[Re(CO)$_3$(H$_2$O)({N7,P$_\beta$}GDP)]$^-$				
S_{Re} $^3J_{H1'-H2'} = 1.0$ Hz[b]	326	−67.8	N	high anti
S_{Re} $^3J_{H1'-H2'} = 4.5$ Hz[b]	325	−66.1	N	high anti
fac-[Re(CO)$_3$(H$_2$O)({N7,P$_\beta$}GDP)]$^-$				
R_{Re} $^3J_{H1'-H2'} = 1.0$ Hz[b]	330	−58.9	N	borderline syn/high anti
R_{Re} $^3J_{H1'-H2'} = 4.5$ Hz[b]	330	−59.1	N	borderline syn/high anti

[a] Data from ref 12. [b] Calculated from lowest-energy models built and minimized in HyperChem.[23]

Table 6. Distances (Å) between H8 Proton and Phosphate Oxygens of *fac*-[Re(CO)$_3$(H$_2$O)({N7,P$_\beta$}GDP)]$^-$ Macrochelate Models

complex	P$_{\alpha(O/pro-\Delta)}$	P$_{\alpha(O/pro-\Lambda)}$	P$_{\alpha(av)}$[a]	P$_{\alpha(O)}$	P$_{\beta(O)}$	P$_{\beta(av)}$[a]
		S_{Re}				
$^3J_{H1'-H2'} = 1.0$ Hz	5.11	5.40	{5.26}	4.49	5.23	{4.86}
$^3J_{H1'-H2'} = 4.5$ Hz	5.18	5.45	5.32	4.54	5.27	{4.91}
		R_{Re}				
$^3J_{H1'-H2'} = 1.0$ Hz	5.72	4.85	{5.28}	6.16	5.25	5.71
$^3J_{H1'-H2'} = 4.5$ Hz	5.78	4.85	5.31	6.19	5.28	5.73

[a] {Values} represent shortest average distances.

signals increased more for ***m*** than for ***M***, while the *fac*-[Re(CO)$_3$(H$_2$O)$_2$({N7}GDP)]$^-$ H8 NMR signal line width remained small in comparison (Supporting Information). This result suggests that the H8 protons of ***M*** and ***m*** are, respectively, farther from and closer to uncoordinated phosphate groups. The distance from H8 to the uncoordinated phosphate group is long for *fac*-[Re(CO)$_3$(H$_2$O)$_2$({N7}GDP)]$^-$, as this signal did not broaden greatly even at high concentrations of Mn^{2+} ion (70 μM).

Because the Mn^{2+} ion titration indicated that phosphate groups are closer to H8 in ***m*** than in ***M*** (see above), we used HyperChem[23] to construct molecular models, allowing us to estimate the distance from H8 to each phosphate oxygen (Table 5). The results obtained are compared to computational results reported for *cis*-[Pt(NH$_3$)$_2$(nucleoside triphosphate)] macrochelate complexes (Table 5).[12,13] On the basis of the pseudorotation phase angle (P, calculated from the endocyclic sugar torsion angles[4]) and the N-glycosidic bond torsion angle (χ, defined by O4′−C1′−N7−C4 values[4]), the 5′-GDP moieties in all four models have N sugars with a high anti orientation (P = 325−330° and χ = −59° to −67°). We should note that these values are comparable to the P and χ values reported for models of *cis*-[Pt(NH$_3$)$_2$({N7,P$_\beta$}-5′-GTP)] (Table 5). The H8−P$_\beta$ distances (Table 6) are shorter for the two S_{Re} models of *fac*-[Re(CO)$_3$(H$_2$O)-({N7,P$_\beta$}GDP)]$^-$ (4.88 Å) than for the two R_{Re} models (5.72 Å). The average H8−P$_\alpha$ distance was ∼5.30 Å for all models (Table 6). Thus, we suggest that ***m*** is the S_{Re} isomer.

Rate Constants of Interchange for TDP, 5′-UDP, and 5′-GDP Products. The rate constants of H$_2$O exchange for *fac*-[Re(CO)$_3$(H$_2$O)$_3$]$^+$ (∼5.5 × 10^{-3} s^{-1}) and *fac*-[Re(CO)$_3$-(H$_2$O)$_2$(OH)] (∼27 s^{-1}) indicate a large range of exchange rates dependent on the coordinated ligand; thus, we assessed the rate constants of interchange between isomers of *fac*-[Re(CO)$_3$(H$_2$O)({P$_\alpha$,P$_\beta$}TDP)]$^-$, *fac*-[Re(CO)$_3$(H$_2$O)({P$_\alpha$,P$_\beta$}-UDP)]$^-$, and *fac*-[Re(CO)$_3$(H$_2$O)({N7,P$_\beta$}GDP)]$^-$ adducts at

Table 7. Rate Constants of Interchange Obtained from ^{1}H−^{1}H ROESY and ^{31}P−^{31}P NOESY Experiments[a]

complex	R	k (s^{-1})
TDP (***M*** pair − ***m*** pair) − P$_\alpha$	3.80	1.08
UDP (***M$_1$*** − ***M$_2$***) − P$_\alpha$	6.37	0.63
UDP (***m$_1$*** − ***m$_2$***) − P$_\alpha$	7.36	0.55
GDP (***M*** − ***m***) − P$_\alpha$	9.51	0.42
GDP (***M*** − ***m***) − H8	6.38	0.63

[a] 25 mM, r = 1:1, pH 3.6, 32 °C.

32 °C.[30] The rate constants of interchange were estimated from ^{1}H−^{1}H ROESY and ^{31}P−^{31}P NOESY experiments at 500 ms mixing time (t_m) (Table 7). The rate constant (k) can be calculated by using the ratio of the relative intensities (peak amplitude, as measured by integration) of the diagonal peaks (I_{AA} and I_{BB}) and the EXSY cross-peaks (I_{AB} and I_{BA}) and the following equation:[31]

$$k = \frac{1}{t_m} \ln\frac{R+1}{R-1} \quad \text{where } R = \frac{(I_{AA} + I_{BB})}{(I_{AB} + I_{BA})}$$

Using ^{31}P−^{31}P NOESY data for the *fac*-[Re(CO)$_3$(H$_2$O)-({P$_\alpha$,P$_\beta$}TDP)]$^-$ and *fac*-[Re(CO)$_3$(H$_2$O)({P$_\alpha$,P$_\beta$}UDP)]$^-$ isomers, we calculated an average k value of ∼0.8 s^{-1} (Table 7). The four isomers of *fac*-[Re(CO)$_3$(H$_2$O)({P$_\alpha$,P$_\beta$}MDP)]$^-$ (Figure 2) can isomerize in four different ways. If either P$_\alpha$ or P$_\beta$ interchanges coordination positions with H$_2$O (and the phosphate oxygen bound to Re(I) does not change), the Re(I) chirality (R_{Re} or S_{Re}) changes to S_{Re} or R_{Re}, respectively. If the change is between O(pro-Δ) and O(pro-Λ) of P$_\alpha$ (Figure 2), with no change in coordination position, then the P$_\alpha$ chirality changes. If both types of interchange occur, for example, via an intermediate in which both O(pro-Δ) and O(pro-Λ) of P$_\alpha$ are bound to Re(I), then both the Re(I) and P$_\alpha$ chiralities change (Figure 8).

The EXSY cross-peak observed between the P$_\alpha$ doublets of the two mirror pairs of *fac*-[Re(CO)$_3$(H$_2$O)({P$_\alpha$,P$_\beta$}TDP)]$^-$ indicates that interchange involves a chirality change only at one chiral center, either Re(I) or P$_\alpha$. Thus, simultaneous changes of both the Re(I) and the P$_\alpha$ chiralities, leading to a synergistic interchange of members of the different mirror pairs, are ruled out.

For *fac*-[Re(CO)$_3$(H$_2$O)({P$_\alpha$,P$_\beta$}UDP)]$^-$, EXSY peaks connect each of the two upfield P$_\alpha$ doublets with the

(30) Salignac, B.; Grundler, P. V.; Cayemittes, S.; Frey, U.; Scopelliti, R.; Merbach, A. E.; Hedinger, R.; Hegetschweiler, K.; Alberto, R.; Prinz, U.; Raabe, G.; Kölle, U.; Hall, S. *Inorg. Chem.* **2003**, *42*, 3516−3526.
(31) Perrin, C. L.; Dwyer, T. J. *Chem. Rev.* **1990**, *90*, 935−967.

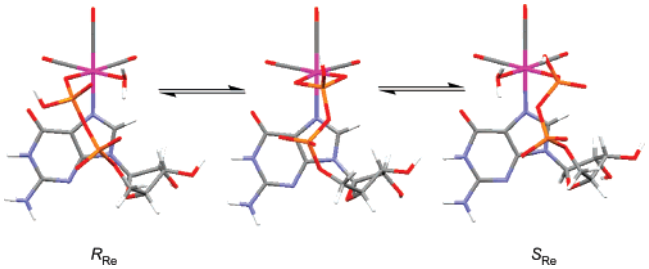

Figure 8. Possible mode of conversion between the R_{Re} and S_{Re} isomers of *fac*-[Re(CO)$_3$(H$_2$O){N7,P$_\beta$}GDP]$^-$.

downfield P$_\alpha$ doublet, but no EXSY peak between the two upfield P$_\alpha$ doublets was detected. Rate constants of interchange calculated from the EXSY peaks for *fac*-[Re(CO)$_3$(H$_2$O)({P$_\alpha$,P$_\beta$}UDP)]$^-$ ($\sim$0.6 s^{-1}) are similar to that found ($\sim$1 s^{-1}) for *fac*-[Re(CO)$_3$(H$_2$O)({P$_\alpha$,P$_\beta$}TDP)]$^-$ isomers (Table 7). These results indicate that interchange among the isomers of *fac*-[Re(CO)$_3$(H$_2$O)({P$_\alpha$,P$_\beta$}UDP)]$^-$ is undoubtedly due to a chirality change at only one chiral center, either Re(I) or P$_\alpha$, as was found for *fac*-[Re(CO)$_3$(H$_2$O)({P$_\alpha$,P$_\beta$}TDP)]$^-$.

Using ^{31}P$-^{31}$P and ^{1}H$-^1$H NOESY data for *fac*-[Re(CO)$_3$(H$_2$O)({N7,P$_\beta$}GDP)]$^-$ (Table 7), we calculated an average *k* of $\sim$0.5 s^{-1} for interchange between the isomers. When P$_\alpha$ is *not* bound to Re(I), as in *fac*-[Re(CO)$_3$(H$_2$O)({N7,P$_\beta$}GDP)]$^-$, there can be only one mechanism for interchange (Figure 3). Interchange of P$_\beta$ and H$_2$O coordination positions (via an intermediate in which two oxygens of P$_\beta$ are bound to Re(I)) leads to a chirality change only at Re(I) (Figure 8).

Because the rate constant for interchange between the R_{Re} and S_{Re} isomers of *fac*-[Re(CO)$_3$(H$_2$O)({N7,P$_\beta$}GDP)]$^-$ is similar to the rate constants for interchange for both *fac*-[Re(CO)$_3$(H$_2$O)({P$_\alpha$,P$_\beta$}TDP)]$^-$ and *fac*-[Re(CO)$_3$(H$_2$O)({P$_\alpha$,P$_\beta$}UDP)]$^-$ isomers, the chirality change at Re(I) for *fac*-[Re(CO)$_3$(H$_2$O)({P$_\alpha$,P$_\beta$}TDP)]$^-$ and *fac*-[Re(CO)$_3$(H$_2$O)({P$_\alpha$,P$_\beta$}UDP)]$^-$ isomers most likely occurs by P$_\beta$ interchanging coordination positions with H$_2$O and *not* by interchange between O(pro-Δ) and O(pro-Λ) of P$_\alpha$ or by P$_\alpha$ interchanging coordination positions with H$_2$O. As mentioned above, this suggested mechanism is supported by the very slow dissociation of 5′-UDP from *fac*-[Re(CO)$_3$(H$_2$O)({P$_\alpha$,P$_\beta$}UDP)]$^-$ adducts, an indication that P$_\beta$ remains bound to Re(I) during isomerization.

Conclusions

The nucleotide adducts described in this study and possessing the *fac*-[Re(CO)$_3$]$^+$ moiety are sufficiently inert to allow the various products to be distinguished by NMR spectroscopy, but the adducts are reactive enough for equilibrium amounts to be assessed. In comparison to studies with other inert metal centers,[7,11] the ^{31}P NMR signals found here are notably sharp, allowing the coupling to be observed. This relatively rare combination of properties allows us to conclude that there is little stereochemical preference for a given diastereomer over other possible diastereomers. Thus, when metal nucleotide complexes act as cofactors with enzymes as part of their natural biochemical function,[6,32−36] the preferred (active) stereochemistry of the metal nucleotide complex is very likely imparted by the enzyme rather than by any intrinsic stereochemical preference dictated by the configuration and geometric parameters of the nucleotide itself. The metals that function in biological roles are generally hard metals such as Mg^{2+}, which have little affinity for the endocyclic nitrogens of nucleotides.[3] Our study suggests that transition metal ions may not have been selected for this role because the affinity of the metal for nitrogen leads to nucleobase binding. The resulting complexes have less metal-to-phosphate interaction compared to other metal−phosphate complexes,[37−39] and thus, the phosphate hydrolysis needed for the biological activity[5] is less favored.

Few other metal centers are likely to possess the useful combination of properties that the *fac*-[Re(CO)$_3$]$^+$ center provides. In addition, unlike some metal centers (e.g., Pt(II) adducts derived from Pt(II) anticancer drugs[37]) the rate of metal-promoted phosphate hydrolysis is very slow, thus avoiding complications in spectral analysis caused by formation of adducts of both the hydrolyzed nucleotide and inorganic phosphate.

Acknowledgment. This investigation was supported by NIH Grant No. GM 29222 (to L.G.M.).

Supporting Information Available: Plots of chemical shift vs pH and area under peak (integral) vs pH for the H8 NMR signals of ***M***, ***m***, *fac*-[Re(CO)$_3$(H$_2$O)$_2$({N7}GDP)]$^-$, and free 5′-GDP^{2-}; plot of line width at full width half-height (fwhh) vs concentration of Mn^{2+} for the H8 NMR signals of ***M***, ***m***, and *fac*-[Re(CO)$_3$(H$_2$O)$_2$({N7}GDP)]$^-$; and plot of chemical shift vs pH for the P$_\beta$ NMR signals of ***M***, ***m***, and *fac*-[Re(CO)$_3$(H$_2$O)$_2$({N7}GDP)]$^-$. This material is available free of charge via the Internet at http://pubs.acs.org.

IC701038F

(32) Cleland, W. W.; Mildvan, A. S. In *Advances in Inorganic Biochemistry*; Eichhorn, G. L., Marzilli, L. G., Eds.; Elsevier/North-Holland: New York, 1979; Vol. 1, pp 163−191.
(33) Dunaway-Mariano, D.; Cleland, W. W. *Biochemistry* **1980**, *19*, 1506−1515.
(34) Lu, Z.; Shorter, A. L.; Dunaway-Mariano, D. *Biochemistry* **1993**, *32*, 2378−2385.
(35) Bakhtina, M.; Lee, S.; Wang, Y.; Dunlap, C.; Lamarche, B.; Tsai, M.-D. *Biochemistry* **2005**, *44*, 5177−5187.
(36) Yang, L.; Arora, K.; Beard, W. A.; Wilson, S. H.; Schlick, T. *J. Am. Chem. Soc.* **2004**, *126*, 8441−8453.
(37) Bose, R. N.; Cornelius, R. D.; Viola, R. E. *Inorg. Chem.* **1984**, *23*, 1181−1182.
(38) Haromy, T. P.; Gilletti, P. F.; Cornelius, R. D.; Sundaralingam, M. *J. Am. Chem. Soc.* **1984**, *106*, 2812−2818.
(39) Haromy, T. P.; Knight, W. B.; Dunaway-Mariano, D.; Sundaralingam, M. *Biochemistry* **1982**, *21*, 6950−6956.